

Mott transition in the Hubbard model on the anisotropic kagome lattice

Yuta Furukawa,¹ Takuma Ohashi,² Yohta Koyama,¹ and Norio Kawakami¹

¹*Department of Physics, Kyoto University, Kyoto 606-8502, Japan*

²*Department of Physics, Osaka University, Toyonaka, Osaka 560-0043, Japan*

(Received 24 June 2010; published 7 October 2010)

We investigate the Mott transition in the anisotropic kagome lattice Hubbard model using the cellular dynamical mean-field theory combined with continuous-time quantum Monte Carlo simulations. By calculating the double occupancy and the density of states, we determine the interaction strength of the first-order Mott transition and show that it becomes small as the anisotropy increases. We also calculate the spin-correlation functions and the single-particle spectrum, and reveal that the quasiparticle and magnetic properties change dramatically around the Mott transition; the spin correlations are strongly enhanced and the quasiparticle bands are deformed. We conclude that such dramatic changes are due to the enhancement of anisotropy associated with the relaxation of frustration around the Mott transition.

DOI: [10.1103/PhysRevB.82.161101](https://doi.org/10.1103/PhysRevB.82.161101)

PACS number(s): 71.30.+h, 71.10.Fd, 71.27.+a

Geometrically frustrated electron systems have provided hot topics in the field of strongly correlated electron systems and have uncovered various new aspects of the Mott transition. The discovery of heavy-fermion behavior in LiV_2O_4 (Refs. 1 and 2) with pyrochlore lattice structure has activated theoretical studies of electron correlations with geometrical frustration.^{3–6} More remarkably, recent experiments on the triangular lattice organic materials κ -(BEDT-TTF)₂X have revealed a spin-liquid ground state in the Mott insulating phase.^{7–11}

The kagome lattice is another prototype of frustrated systems, which shares some essential properties with other frustrated lattices. The localized electron systems on this lattice have been intensively studied and many unusual properties have been found.¹² In particular, a spin-liquid state observed in the herbertsmithite $\text{ZnCu}_3(\text{OH})_6\text{Cl}_2$ with kagome lattice structure^{13,14} has received considerable attention. A related spinel oxide $\text{Na}_4\text{Ir}_3\text{O}_8$ with hyperkagome structure, which is a three-dimensional analog of kagome lattice, is also proposed as a candidate for the spin liquid.^{15,16} The issue of electron correlations on the kagome lattice was addressed by applying the fluctuation exchange (FLEX) approximation¹⁷ and the quantum Monte Carlo (QMC) method¹⁸ to the Hubbard model. Also in our recent study, we found a heavy Fermi-liquid state emerging in a metallic phase near the Mott transition by using the cellular dynamical mean-field theory (CDMFT).¹⁹ Furthermore, an idea of chirality-spin separation was proposed to explain low-energy characteristic properties.²⁰ In spite of such intensive theoretical investigations, however, the effects of spatial anisotropy have not yet been addressed. The systematic exploration of the anisotropy is desired to elucidate how the frustration affects the nature of Mott transition, the quasiparticle formation, the magnetic properties, etc. It has indeed been clarified that in a moderately frustrated system on the anisotropic triangular lattice, the Mott transition shows a reentrant behavior,^{9,21,22} where the low-temperature transition is governed by the enhanced antiferromagnetic (AFM) correlations. This is a unique feature that may occur neither in the unfrustrated square lattice²³ nor in the fully frustrated triangular lattice.²⁴ This naturally motivates us to study the effects of frustration on

the Mott transition by systematically controlling the spatial anisotropy.

In this Rapid Communication, we study the Mott transition in the Hubbard model on the anisotropic kagome lattice by means of CDMFT (Ref. 25) combined with the continuous-time QMC (CT-QMC) method.²⁶ We first treat the isotropic system to confirm our previous results studied with a slightly different method.¹⁹ As the anisotropy is introduced, electronic properties drastically change around the Mott transition; the spin correlations are strongly enhanced and the quasiparticle bands are deformed substantially even if the system is slightly away from the isotropic point. We elucidate that such dramatic changes are due to the enhancement of anisotropy driven by the relaxation of frustration around the Mott transition.

We consider the Hubbard model on the anisotropic kagome lattice. Here, we set the lattice geometry as a square form, where the first Brillouin zone is $-\pi < k_x, k_y < \pi$.¹⁷ The Hamiltonian reads

$$H = -t \sum_{\langle i,j \rangle, \sigma} c_{i\sigma}^\dagger c_{j\sigma} - t' \sum_{(i,j), \sigma} c_{i\sigma}^\dagger c_{j\sigma} + U \sum_i n_{i\uparrow} n_{i\downarrow}, \quad (1)$$

where $c_{i\sigma}^\dagger$ ($c_{j\sigma}$) creates (annihilates) an electron with spin σ at site i and $n_{i\sigma} = c_{i\sigma}^\dagger c_{i\sigma}$. The hopping integrals and the Hubbard interaction are denoted by t (t') and U , respectively. The system corresponds to the fully frustrated kagome lattice at $t'/t=1$, and frustration becomes weaker with decreasing t'/t . The end member at $t'/t=0$ is called a decorated square lattice or Lieb²⁷ lattice. We choose the energy unit as $t=1$ hereafter. To investigate strong correlations and geometrical effects, we use CDMFT,²⁵ a cluster extension of DMFT.²⁸ CDMFT has been successfully applied to a lot of frustrated electron systems so far.^{19–22,24,29,30}

In CDMFT, the original lattice problem is mapped onto an effective cluster problem. Each unit cell of the anisotropic kagome lattice has three sites. We thus end up with a three-site cluster model coupled to a self-consistently determined medium. Note that in the isotropic kagome lattice Hubbard model, the cluster size dependence has been discussed and the results for the three-site cluster CDMFT are in very good agreement with those for the larger cluster (nine site)

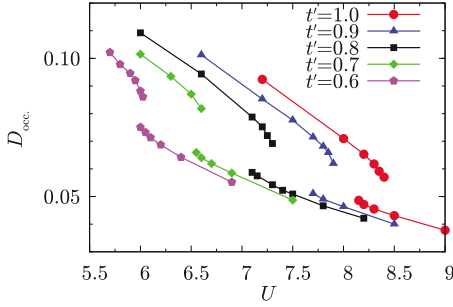


FIG. 1. (Color online) Double occupancy as a function of interaction strength U for several t' at $T=0.05$.

CDMFT.²⁰ Given the Green's function for the effective medium, \hat{G} , we compute the cluster Green's function \hat{G} and the cluster self-energy $\hat{\Sigma}$ in the effective cluster model, where \hat{O} denotes a 3×3 matrix. To calculate \hat{G} and $\hat{\Sigma}$ in the effective cluster model, we use the hybridization-expansion CT-QMC method.²⁶ In this method, a sign problem can appear even in the half-filled model on the bipartite clusters. The sign problem strongly depends on the choice of basis set in the local Hamiltonian. We choose the basis set which diagonalizes the local hopping matrix \hat{t}_{loc} written in the sublattice basis,

$$\hat{t}_{\text{loc}} = \begin{pmatrix} 0 & t & t \\ t & 0 & t' \\ t & t' & 0 \end{pmatrix}. \quad (2)$$

We find that this choice substantially reduces the sign problem in QMC simulations. By using this basis set, the QMC samples which shows a minus sign is reduced to less than 1% of the total QMC samples for the isotropic kagome lattice and for $t'=0.6$, it is at most 35%. We iterate the DMFT self-consistent loop until the convergence of this procedure is achieved within 50 iterations at most. In each iteration, we typically use 2.5×10^7 QMC sweeps to reach sufficient computational accuracy at very low temperature, $T=0.05$.

Let us now investigate the Mott transition on the anisotropic kagome lattice at half filling. In order to find evidence of the Mott transition, we calculate the U dependence of the double occupancy $D_{\text{occ.}} = \frac{1}{3} \sum_{m=1}^3 \langle n_m \uparrow n_m \downarrow \rangle$ for various t' . The double occupancy monotonically decreases with increasing U and shows a discontinuous jump at the interaction U_c , as shown in Fig. 1. We also find hysteresis, which signals the emergence of the first-order Mott transition. In the isotropic kagome system for $t'=1.0$, the Mott transition occurs at fairly large interaction strength $U_c \sim 8.4$ compared with the bandwidth $W=6$. This is consistent with our previous study using CDMFT combined with Hirsch-Fye QMC.¹⁹ In anisotropic cases, the interaction strength U_c becomes small as t' decreases. The location of the critical end points is roughly estimated as $(U, T) \sim (8.1, 0.08)$, $(7.2, 0.08)$, and $(6.0, 0.05)$ for $t'=1.0, 0.8,$ and 0.6 , respectively. Note that the bandwidth $W/t = 4\sqrt{2} \sim 5.66$ for $t'=0$ and the reduction in W is less than 6%. Therefore, we can say that the metallic region shrinks as geometrical frustration is weakened.

To see the metal-insulator transition more clearly,

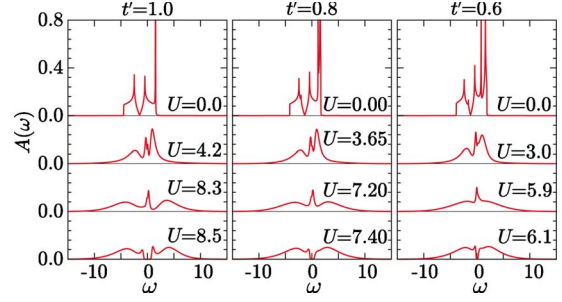


FIG. 2. (Color online) Density of states for typical U and t' at $T=0.05$.

we calculate the density of states (DOS) $A(\omega) = -\frac{1}{3\pi} \sum_{m=1}^3 \text{Im} G_{mm}(\omega + i\delta)$ by applying the maximum entropy method (MEM) (Ref. 31) to the imaginary-time QMC data. In Fig. 2, we show the DOS for $t'=1.0, 0.8,$ and 0.6 . We clearly see that the insulating gap opens around the Fermi level in the large U region beyond U_c . For $t'=1.0$, the three bands are strongly renormalized and the heavy quasiparticle states having a sharp peak in the DOS emerge near the Fermi level in the strong correlation regime. A similar peak structure also appears for $t'=0.8, 0.6$ in the weaker U region than that for $t'=1.0$. We note here that MEM generally has a tendency to amplify errors so that the results obtained should be carefully analyzed. We have checked that the results of DOS obtained by MEM are consistent with those estimated by the double occupancy, etc., so that they may provide supplementary information for the Mott transition.

Let us now turn to the magnetic correlations. To see how frustration affects them around the Mott transition, we calculate the nearest-neighbor (NN) spin-correlation function $\langle S_i^z S_{i+1}^z \rangle$. We compute $\langle S_i^z S_{i+1}^z \rangle$ in the effective cluster model. Here, i denotes a sublattice index. The NN bonds 1-2 and 1-3 are connected by the hopping integral t and the other NN bond 2-3 is connected by t' . In Fig. 3, we show $\langle S_i^z S_{i+1}^z \rangle$ as a function of U for several t' . In the isotropic case, $\langle S_1^z S_2^z \rangle$, $\langle S_1^z S_3^z \rangle$, and $\langle S_2^z S_3^z \rangle$ are equivalent and have small negative

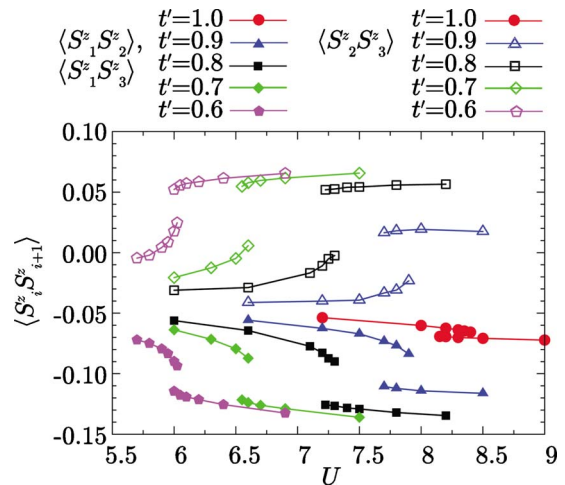


FIG. 3. (Color online) Nearest-neighbor spin-correlation function $\langle S_i^z S_{i+1}^z \rangle$ as a function of U for several t' , where the suffix i specifies a sublattice.

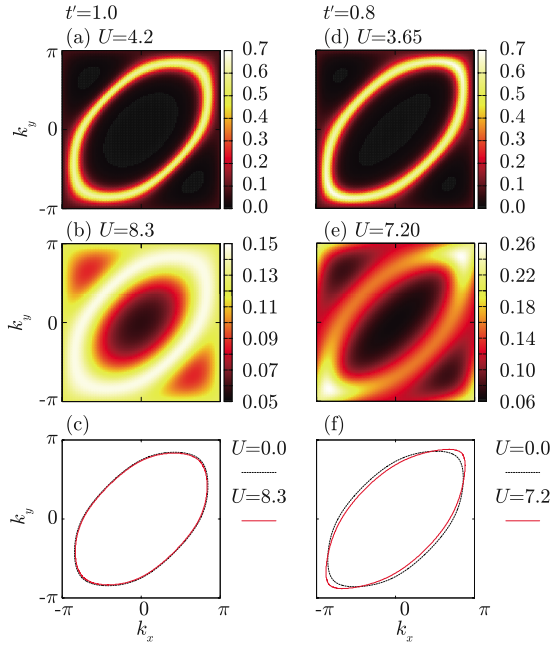


FIG. 4. (Color online) Momentum-resolved spectral weight at the Fermi level. In (c) and (f), we show the Fermi surfaces deduced from (b) and (e) together with those for the noninteracting case for reference.

values for any U . This indicates that the AFM spin correlation is suppressed due to the strong frustration. As finite anisotropy is introduced ($t'=0.9, 0.8, 0.7, 0.6$), the spin correlations dramatically change near the Mott transition; $\langle S_1^x S_2^x \rangle$ and $\langle S_1^y S_2^y \rangle$ show strong AFM correlations while $\langle S_1^z S_2^z \rangle$ tends to be ferromagnetic. These behaviors indicate the tendency to a ferrimagnetic ordering (or an AFM-type ordering on a decorated square lattice). We thus find that magnetic properties in the system are very sensitive to the anisotropy, whose effect is particularly enhanced in the vicinity of the Mott transition point.

The relaxation of frustration strongly affects the formation of quasiparticle bands. We next investigate the momentum-resolved spectral weight at the Fermi level $A(\mathbf{k}, \omega=0)$ in the metallic phase. Using the cluster self-energy, we obtain the \mathbf{k} -dependent Green's function,

$$G_{mn}(\mathbf{k}, \omega) = e^{i\mathbf{k} \cdot (\mathbf{r}_m - \mathbf{r}_n)} [\omega + \mu - \hat{\epsilon}(\mathbf{k}) - \hat{\Sigma}(\omega)]_{mn}^{-1} \quad (3)$$

and $A(\mathbf{k}, \omega=0) = -\frac{1}{3\pi} \sum_{m=1}^3 \text{Im} G_{mm}(\mathbf{k}, \omega=0)$. Here, we approximately compute $A(\mathbf{k}, \omega=0)$ as $A(\mathbf{k}, \omega=0) \sim -\frac{1}{3\pi} \sum_{m=1}^3 \text{Im} G_{mm}(\mathbf{k}, i\omega_n \rightarrow 0)$. In Fig. 4, we show color plots of $A(\mathbf{k}, \omega=0)$. Also, shown in Figs. 4(c) and 4(f) is the Fermi surface deduced from the trajectory of their peaks. In the isotropic case, $A(\mathbf{k}, \omega=0)$ for $U=4.2$ has strong intensity at the Fermi surface and the profile of the Fermi surface is consistent with that in the noninteracting case. Near the Mott transition, for $U=8.3$, the Fermi surface keeps the same shape as in the noninteracting case, although the quasiparticle peak in $A(\mathbf{k}, \omega)$ is somewhat obscured at finite temperatures. In contrast, for $t'=0.8$, the geometry of the Fermi surface changes near the Mott transition. In the weak-coupling

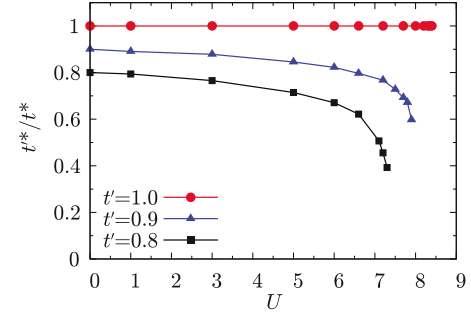


FIG. 5. (Color online) Ratio of the effective hopping integrals t^{**} and t^* as a function of U in the metallic phase.

regime, for $U=3.65$, the Fermi surface has a shape similar to that in the noninteracting case. As U increases, for $U=7.2$, the shape becomes elongated and quite different from that in the noninteracting case. It is known that the shape of the noninteracting Fermi surface is elongated along the $k_x=k_y$ direction as t' decreases.¹⁷ Therefore, we find that the band structure of quasiparticles becomes much more anisotropic due to the enhancement of hopping anisotropy, which is induced by the relaxation of frustration. Note that the \mathbf{k} dependence of $A_{\mathbf{k}}(0)$ at the Fermi surface in Fig. 4(e) is due to the contribution of the upper band rather than the central band which constructs the Fermi surface. Around the Mott transition, the contribution of the upper band to the spectral weight at the Fermi surface with the maximum weight near $(k_x, k_y) \sim (\pm\pi, \pm\pi)$ becomes large while the \mathbf{k} dependence of the spectral weight at the Fermi surface of the central band is small. This induces the \mathbf{k} dependence of $A_{\mathbf{k}}(0)$. This behavior is consistent with the previous results by the FLEX approximation.¹⁷

In order to confirm the above scenario, we investigate the renormalization of hopping integrals. In the low-energy limit, the Green's function in the effective cluster model may be given by

$$\hat{G}(\omega) = \hat{Z}^{1/2} [(\omega + \mu) \hat{1} - \hat{t}_{\text{loc}}^* - \hat{\Delta}^*(\omega)]^{-1} \hat{Z}^{1/2}, \quad (4)$$

where \hat{t}_{loc}^* is the matrix representation of the renormalized hopping integrals defined by $\hat{t}_{\text{loc}}^* = \hat{Z}^{1/2} [\hat{t}_{\text{loc}} - \text{Re} \hat{\Sigma}(\omega=0)] \hat{Z}^{1/2}$, where $\hat{Z} = [\hat{1} - \partial \text{Re} \hat{\Sigma}(\omega) / \partial \omega |_{\omega=0}]^{-1}$. In \hat{t}_{loc}^* , the original hopping integral t (t') is renormalized as $t \rightarrow t^*$ ($t' \rightarrow t'^*$). The renormalized hybridization function is defined similarly: $\hat{\Delta}^*(\omega) = \hat{Z}^{1/2} \hat{\Delta}(\omega) \hat{Z}^{1/2}$.

In Fig. 5, we show the U dependence of the ratio of the renormalized hopping integrals t'^*/t^* . In the isotropic case, t'^*/t^* is always unity due to the symmetry requirement, giving rise to strong frustration near the Mott transition. For the anisotropic cases of $t'/t=0.9$ and 0.8 , t'^*/t^* does not show any drastic change in the small U region. However, in the vicinity of the Mott transition, t'^*/t^* rapidly decreases, implying that the anisotropy in hopping integrals is considerably enhanced there. As a result, geometrical frustration becomes weak. In other words, strong frustration developed in the nearly isotropic models triggers the strong renormalization of anisotropic hopping in the vicinity of the Mott tran-

sition. The enhanced anisotropy deforms the band structures and develops the spin correlations. We thus conclude that the origin of the dramatic changes found around the Mott transition is the enhancement of anisotropy in the hopping integral associated with the relaxation of frustration. We note that the above mechanism for relaxation of frustration may be generic for frustrated electron systems in the vicinity of the Mott transition. For example, the reentrant Mott transition found for the anisotropic triangular lattice compound⁹ may be caused by the above mechanism. Namely, if the lattice anisotropy is weak, a metallic state near the Mott transition keeps the isotropic nature approximately in the weak-coupling regime (high temperature) and thus behaves as a fully frustrated model. However, as the temperature is lowered, the system enters the strong-coupling regime, where the anisotropy is enhanced and the AFM correlations are developed. This may trigger the reentrant Mott transition where the low-temperature Mott phase is accompanied by enhanced AFM correlations.

In summary, we have studied the Mott transition in the

Hubbard model on the anisotropic kagome lattice by means of the CDMFT combined with CT-QMC. For anisotropic lattice systems, we have found that the quasiparticle and magnetic properties drastically change around the Mott transition; the spin correlations get strongly enhanced and the quasiparticle bands are deformed. It has been elucidated that these behaviors are due to the relaxation of frustration caused by the enhancement of anisotropy around the Mott transition.

The authors thank Ansugur Liebsch for valuable discussions. A part of numerical computations was done at the Supercomputer Center at ISSP, University of Tokyo and also at YITP, Kyoto University. This work was supported by KAKENHI (Grants No. 21740232, No. 20104010, No. 21540359, and No. 20102008), the Next Generation Super Computing Project “Nanoscience Program” from the MEXT of Japan, the Grant-in-Aid for the Global COE Programs “The Next Generation of Physics, Spun from Universality and Emergence” from MEXT of Japan, and JSPS through its FIRST Program.

-
- ¹S. Kondo *et al.*, *Phys. Rev. Lett.* **78**, 3729 (1997).
²P. E. Jönsson, K. Takenaka, S. Niitaka, T. Sasagawa, S. Sugai, and H. Takagi, *Phys. Rev. Lett.* **99**, 167402 (2007).
³Y. Imai and N. Kawakami, *Phys. Rev. B* **65**, 233103 (2002).
⁴R. Arita, K. Held, A. V. Lukoyanov, and V. I. Anisimov, *Phys. Rev. Lett.* **98**, 166402 (2007).
⁵T. Yoshioka, A. Koga, and N. Kawakami, *Phys. Rev. B* **78**, 165113 (2008).
⁶K. Hattori and H. Tsunetsugu, *Phys. Rev. B* **79**, 035115 (2009).
⁷S. Lefebvre, P. Wzietek, S. Brown, C. Bourbonnais, D. Jérôme, C. Mézière, M. Fourmigué, and P. Batail, *Phys. Rev. Lett.* **85**, 5420 (2000).
⁸Y. Shimizu, K. Miyagawa, K. Kanoda, M. Maesato, and G. Saito, *Phys. Rev. Lett.* **91**, 107001 (2003).
⁹F. Kagawa, T. Itou, K. Miyagawa, and K. Kanoda, *Phys. Rev. B* **69**, 064511 (2004).
¹⁰T. Kashima and M. Imada, *J. Phys. Soc. Jpn.* **70**, 3052 (2001).
¹¹T. Yoshioka, A. Koga, and N. Kawakami, *Phys. Rev. Lett.* **103**, 036401 (2009).
¹²G. Misguich and C. Lhuillier, in *Frustrated Spin Systems*, edited by H. T. Diep (World Scientific, Singapore, 2004).
¹³J. S. Helton *et al.*, *Phys. Rev. Lett.* **98**, 107204 (2007).
¹⁴P. Mendels, F. Bert, M. A. de Vries, A. Olariu, A. Harrison, F. Duc, J. C. Trombe, J. Lord, A. Amato, and C. Baines, *Phys. Rev. Lett.* **98**, 077204 (2007).
¹⁵Y. Okamoto, M. Nohara, H. Aruga-Katori, and H. Takagi, *Phys. Rev. Lett.* **99**, 137207 (2007).
¹⁶Y. Zhou, P. A. Lee, T.-K. Ng, and F.-C. Zhang, *Phys. Rev. Lett.* **101**, 197201 (2008).
¹⁷Y. Imai, N. Kawakami, and H. Tsunetsugu, *Phys. Rev. B* **68**, 195103 (2003).
¹⁸N. Bulut, W. Koshibae, and S. Maekawa, *Phys. Rev. Lett.* **95**, 037001 (2005).
¹⁹T. Ohashi, N. Kawakami, and H. Tsunetsugu, *Phys. Rev. Lett.* **97**, 066401 (2006).
²⁰M. Udagawa and Y. Motome, *Phys. Rev. Lett.* **104**, 106409 (2010).
²¹T. Ohashi, T. Momoi, H. Tsunetsugu, and N. Kawakami, *Phys. Rev. Lett.* **100**, 076402 (2008).
²²A. Liebsch, H. Ishida, and J. Merino, *Phys. Rev. B* **79**, 195108 (2009).
²³T. Maier, M. Jarrell, T. Pruschke, and M. H. Hettler, *Rev. Mod. Phys.* **77**, 1027 (2005).
²⁴O. Parcollet, G. Biroli, and G. Kotliar, *Phys. Rev. Lett.* **92**, 226402 (2004).
²⁵G. Kotliar, S. Y. Savrasov, G. Pálsson, and G. Biroli, *Phys. Rev. Lett.* **87**, 186401 (2001).
²⁶P. Werner and A. J. Millis, *Phys. Rev. B* **74**, 155107 (2006).
²⁷E. H. Lieb, *Phys. Rev. Lett.* **62**, 1201 (1989).
²⁸A. Georges, G. Kotliar, W. Krauth, and M. J. Rozenberg, *Rev. Mod. Phys.* **68**, 13 (1996).
²⁹B. Kyung and A.-M. S. Tremblay, *Phys. Rev. Lett.* **97**, 046402 (2006).
³⁰D. Galanakis, T. D. Stanescu, and P. Phillips, *Phys. Rev. B* **79**, 115116 (2009).
³¹M. Jarrell and J. E. Gubernatis, *Phys. Rep.* **269**, 133 (1996).